

Helical structure, stability, and dynamics in human apolipoprotein E3 and E4 by hydrogen exchange and mass spectrometry

Palaniappan S. Chetty^a, Leland Mayne^b, Sissel Lund-Katz^a, S. Walter Englander^{b,1}, and Michael C. Phillips^{a,1}

^aDivision of Translational Medicine and Human Genetics, Perelman School of Medicine at the University of Pennsylvania, Philadelphia, PA 19104-5158; and ^bThe Johnson Research Foundation, Department of Biochemistry and Biophysics, Perelman School of Medicine at the University of Pennsylvania, Philadelphia, PA 19104

Contributed by S. Walter Englander, December 19, 2016 (sent for review October 24, 2016; reviewed by Carl Frieden and Robert O. Ryan)

Apolipoprotein E (apoE) plays a critical role in cholesterol transport in both peripheral circulation and brain. Human apoE is a polymorphic 299-residue protein in which the less common E4 isoform differs from the major E3 isoform only by a C112R substitution. ApoE4 interacts with lipoprotein particles and with the amyloid- β peptide, and it is associated with increased incidence of cardiovascular and Alzheimer's disease. To understand the structural basis for the differences between apoE3 and E4 functionality, we used hydrogen-deuterium exchange coupled with a fragment separation method and mass spectrometric analysis to compare their secondary structures at near amino acid resolution. We determined the positions, dynamics, and stabilities of the helical segments in these two proteins, in their normal tetrameric state and in mutation-induced monomeric mutants. Consistent with prior X-ray crystallography and NMR results, the N-terminal domain contains four α -helices, 20 to 30 amino acids long. The C-terminal domain is relatively unstructured in the monomeric state but forms an α -helix \sim 70 residues long in the self-associated tetrameric state. Helix stabilities are relatively low, 4 kcal/mol to 5 kcal/mol, consistent with flexibility and facile reversible unfolding. Secondary structure in the tetrameric apoE3 and E4 isoforms is similar except that some helical segments in apoE4 spanning residues 12 to 20 and 204 to 210 are unfolded. These conformational differences result from the C112R substitution in the N-terminal helix bundle and likely relate to a reduced ability of apoE4 to form tetramers, thereby increasing the concentration of functional apoE4 monomers, which gives rise to its higher lipid binding compared with apoE3.

apolipoprotein E | hydrogen exchange mass spectrometry | cholesterol | protein secondary structure | amphipathic helix

Apolipoprotein E (apoE) is a protein of major biological and medical importance. It is expressed in multiple tissues, including liver and brain. It is a member of the exchangeable apolipoprotein gene family, a structural component of lipoprotein particles, and a key regulator of lipoprotein metabolism and cholesterol transport. Human apoE is a 299-residue protein with multiple amphipathic α -helical repeats that confer functionality (1, 2). Three major isoforms exist—E2, E3, and E4—each differing by a single amino acid substitution. The parent apoE3 contains cysteine at position 112 and arginine at position 158. ApoE2 has cysteine at both of these sites, and E4 has arginine at both (1). The allele frequencies of ϵ 2, ϵ 3, and ϵ 4 in the human population are 7%, 78%, and 14%, respectively (3).

ApoE solubilizes and transports lipids in the peripheral circulation and promotes clearance of triglyceride-rich lipoprotein particles by ligating to members of the low-density lipoprotein receptor (LDLR) family (1, 4). ApoE2 and E4 polymorphism leads to hyperlipidemia and increased risk of cardiovascular disease. Thus, apoE2, which contains the amino acid change R158C located near the LDLR recognition site, binds poorly to the LDLR (1), inhibiting clearance of triglyceride-rich lipoprotein remnant particles from the circulation (5, 6). ApoE2 is associated with the occurrence of type III hyperlipoproteinemia. The C112R substitution in apoE4 modifies its lipid and lipoprotein

binding properties so that it binds much better than apoE3 to very-low-density lipoprotein (VLDL) particles (7). This disrupts the lipolysis cascade involved in the catabolism of VLDL and impairs its clearance, producing higher plasma cholesterol levels and increased risk of cardiovascular disease (3, 8). In addition, the expression of apoE4 in the brain is the major genetic risk factor for early onset Alzheimer's disease (9, 10). ApoE4 leads to reduced clearance of extracellular amyloid plaque deposits in the brain (10), increases neuronal degeneration (11), and reduces longevity (12). It is known that apoE can bind to amyloid- β peptide (13), but further mechanistic detail is lacking.

A critical question concerns how the single amino acid C112R change in apoE4 affects protein structure or dynamics to cause these profound physiological and pathological variations. Despite much research, detailed structural information is lacking. A high-resolution structure of the wild-type (WT) apoE molecule is unavailable because both apoE3 and E4 self-associate through their C-terminal domains to form a tetramer, which has inhibited study by X-ray crystallography and NMR. It has been possible to obtain the structures of the N- and C-terminal domains using a monomeric variant with five mutations (F257A/W264R/V269A/L279Q/V287E) in the C-terminal domain that interfere with tetramer formation while maintaining similar lipid-binding activity (14, 15). NMR study of the monomeric variant of human apoE3 (16) and crystallography of the isolated N-terminal domain (1, 17) show that residues 23–167 form an N-terminal antiparallel four-helix bundle. The structure of the functionally important C-terminal domain in WT apoE is unknown. It is thought to contain α -helices that form an exposed

Significance

Apolipoprotein E (apoE) serves as a cholesterol transport protein in both the peripheral circulation and the brain. In humans, the less common apoE4 isoform, which differs from the most abundant parent apoE3 by a single C112R substitution, is associated with increased incidence of cardiovascular disease and Alzheimer's disease. To understand the structural basis for the altered functionality, we used hydrogen exchange mass spectrometry to compare the structure, stability, and molecular dynamics of these isoforms. The C112R substitution in apoE4 leads to unfolding of certain helical segments that reduces self-association and is expected to enhance the binding of apoE4 to triglyceride-rich lipoprotein particles in plasma and to amyloid- β deposits in the brain.

Author contributions: P.S.C., L.M., S.L.-K., S.W.E., and M.C.P. designed research; P.S.C. and S.L.-K. performed research; L.M., S.W.E., and M.C.P. analyzed data; and S.W.E. and M.C.P. wrote the paper.

Reviewers: C.F., Washington University School of Medicine; and R.O.R., Children's Hospital Oakland Research Institute.

The authors declare no conflict of interest.

¹To whom correspondence may be addressed. Email: engl@mail.med.upenn.edu or mcp3@mail.med.upenn.edu.

This article contains supporting information online at www.pnas.org/lookup/suppl/doi:10.1073/pnas.1617523114/-DCSupplemental.

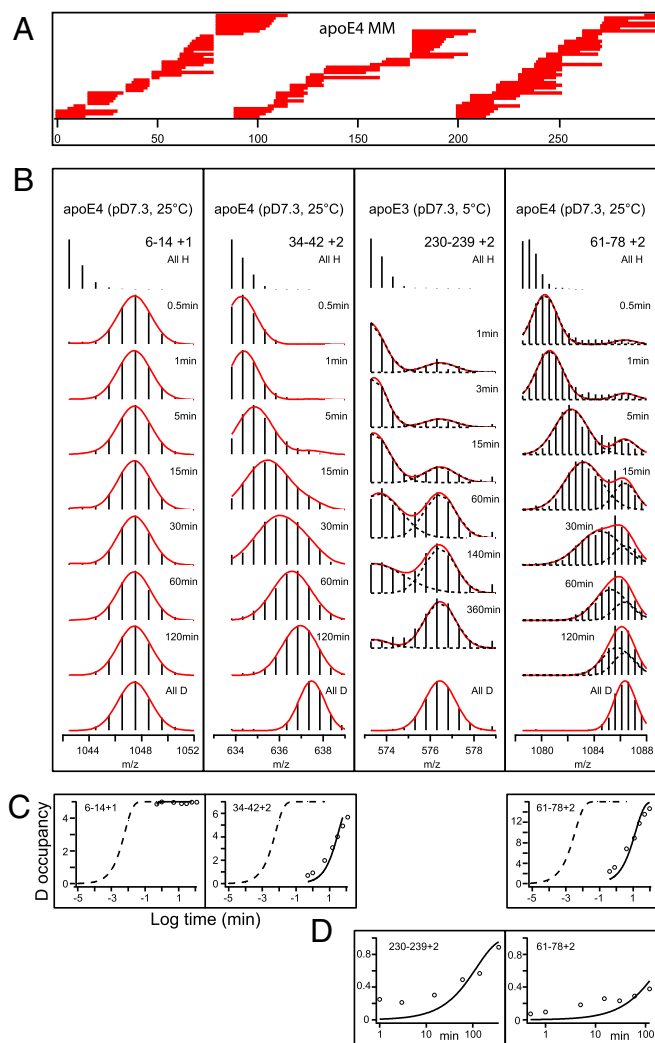


Fig. 1. Illustration of HX MS data. (A) Peptide map showing the ~115 useful unique peptide fragments obtained for the 299-residue apoE4 monomolecular mutant. H-to-D exchange results measured for individual peptides, as in *B–D*, reveal the time-dependent HX behavior for the corresponding segment in the protein. (B) MS isotopic envelopes (left to right) a peptide that exchanges too fast to measure, a pure EX2 case, a pure EX1 case, and a peptide that experiences both EX2 and EX1 HX reactions. (C) EX2 HX versus time for the peptide segments shown. For each peptide, EX2 exchange parallels the reference curve (dashed line; $P_f = 1$), showing that the entire segment exchanges by way of the same unfolding reaction. The multiplicative offset on the $\log(\text{time})$ axis gives the P_f and thus the ΔG for the operative unfolding reaction. (D) EX1 results are plotted as the time-dependent increase in the heavier population fraction, indicating the fraction of the population that has exchanged (opened at least once) during the experimental HX time.

hydrophobic surface that mediates the self-association of apoE in a monomer–tetramer equilibrium (18), its binding to phospholipid in lipoprotein particles (19–21), and its interaction with amyloid- β (13).

In the monomeric apoE3 variant, the C domain interacts with the N-terminal helix bundle domain through hydrogen bonds and salt bridges (16), especially involving the juxtaposition of residues 271–279 in the C domain with helix 4 (residues 131–164) in the N-domain bundle (22, 23). Interaction of apoE with lipid surfaces is initiated by the C domain (24). Whereas the lipid-free apoE3 and E4 tetramers do not interact with the LDLR because the binding site in N-domain helix 4 is masked, lipid-bound apoE in which the N-terminal helix bundle is opened (19, 20) does interact (1). Importantly, the apoE4 C112R substitution is located in helix 3 (residues 89–125) of the N-terminal helix bundle, but the substitution

also alters lipid-binding activity mediated by the C-terminal domain. This parallelism occurs because of altered domain–domain interactions in the apoE3 and E4 isoforms, variously explained by either altered salt-bridge formation (25) or allosteric effects (22, 23, 26). The bulky charged arginine residue in apoE4 acts directly to destabilize the N-terminal helix bundle and, indirectly, the C-terminal domain (15, 27).

Various studies have established that the organization and properties of the C-terminal domain are different in apoE3 and apoE4 (8, 28, 29). To better understand the structural basis for the differences in isoform behavior, we compared helix structure, stability, and dynamics in WT apoE3 and apoE4, and examined the consequences of the five mutations associated with formation of both monomer variants. We applied hydrogen exchange mass spectrometry (HX MS) methodology as in our previous studies of the related apoA-I molecule (30–33). The results show that the C112R substitution that distinguishes apoE4 from apoE3 leads to destabilization of certain helical segments in both the N and C domains of the protein in the tetrameric state. These structural changes alter the monomer–tetramer and the monomer to lipid and to amyloid- β equilibria so that, relative to apoE3, more functionally active apoE4 monomer is present. As a consequence, apoE4 binds more than apoE3 to lipid and amyloid- β surfaces—differences that likely underlie the greater disease risk associated with the former isoform.

Because apoE exchanges between lipoprotein particles in plasma *in vivo* (4, 6), there is a water-soluble pool of lipid-free protein, and, based on its self-association properties (18, 34), it is expected to be predominantly tetrameric at concentrations down to the 0.1- μM range. This pool of plasma apoE has been identified and designated HDL-LpE (35). In normolipidemic individuals, its concentration is ~0.2 μM and it accounts for ~20% of total plasma apoE. Pre- β 1-HDL-LpE is a lipid-free, apoE-only (no apoA-I) particle of the same size as apoE tetramer (hydrodynamic diameter \approx 12 nm), and it is active in the transfer of apoE to triglyceride-rich lipoprotein particles. Therefore, elucidation of the effect of the C112R substitution on apoE tetramer structure and stability is significant for better understanding the role of apoE polymorphism in lipoprotein metabolism.

Results and Discussion

HX Kinetics and ApoE Secondary Structure. The apoE variants studied here are the WT and the monomeric mutants (MMs) of apoE3 and apoE4, at pD (pH measured in D_2O) 7.3 and 25 °C, and at 5 °C to allow measurement of less HX-protected, faster exchanging sites. Fig. 1A shows the collection of overlapping peptides, well over 100, typically obtained in the measurement of H-to-D exchange time points for all variants. Each peptide monitors the protein segment indicated. Comparison of results for overlapping peptides provides many internal consistency checks and often allows HX behavior to be resolved to subpeptide level. Fig. 1B illustrates HX MS data that display the different kinds of HX behaviors observed at different apoE regions, variously EX1, EX2, or mixed EX1+EX2 kinetics as explained in *SI Appendix*. It is useful to visualize time-dependent HX as in Fig. 1C for EX2 behavior and in Fig. 1D for EX1 behavior. The EX2 data shown, plotted on a $\log(\text{time})$ scale, parallel the reference curve for that peptide (dashed line, computed for the same sequence in random coil). This parallelism shows that all (or many) of the amide sites exchange by the same cooperative unfolding reaction, and allows the HX protection factor (P_f), and therefore the stability of the helix, to be calculated from the degree of the rate shift (see *SI Appendix*). The complete HX MS kinetic data sets are presented in *SI Appendix*. They were analyzed using procedures summarized in *Materials and Methods* and *SI Appendix*, and described before in detail for apoA-I (31). Quantitative rate results for the different apoE variants studied are in *SI Appendix*, Tables S1–S4.

HX results obtained for many overlapping peptides make it possible to determine helix locations within each type of apoE molecule. As an example, Fig. 2 shows results that place the N-terminal helix of the MM apoE4MM. The amide NHs in peptide

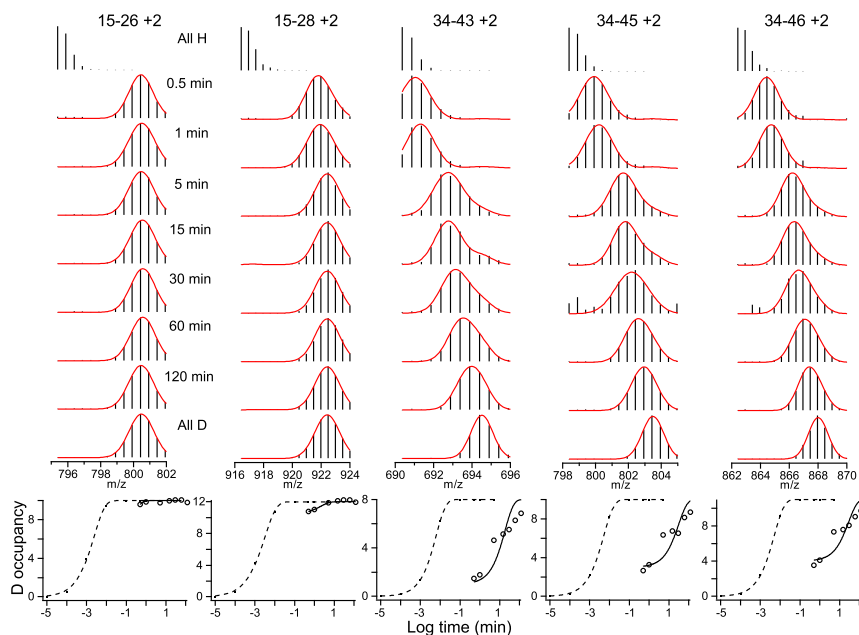


Fig. 2. Mass spectra of apoE4MM peptide fragments (charge state +2) and their increase in mass as a function of H-to-D exchange time (pD 7.3, 25 °C). The five overlapping peptides span the protein sequence between amino acids 15 and 46 and specify the position of a helix between residues 22 and 41, as described in *Comparison of Helix Locations in Tetrameric WT ApoE3 and ApoE4*. The helix exchanges by a whole-helix unfolding reaction in an EX2 mode (reclosing is faster than the intrinsic HX time constant). HX time-point samples for each peptide were corrected for back exchange measured for fully D samples. These and other overlapping peptides define the first helix as residues 22–41.

15–26 are all unprotected. In peptide 15–28, longer by two residues, there are two protected amide hydrogens consistent with protection against HX at residues 27 and 28. It follows that the amide NH of residue 27 is hydrogen bonded to the main chain carbonyl of residue 23 (i to i-4). Residues 24, 25, and 26 form the first turn of the helix with their amide hydrogens not protected by hydrogen bond acceptors and so exchange rapidly. Further along the helix, the three peptide fragments 34–43, 34–45 and 34–46 all contain seven protected amide NH and, respectively, two, three, and four unprotected amide NH as the peptide elongates, indicating that H-bonded helix protection terminates at about residue 41. Therefore, the first α -helix in apoE4MM extends between residues 22 and 41(\pm 2). Application of this analysis to the entire data set for apoE4MM indicates that the molecule contains three more α -helices located between residues 55 and 73, 97 and 120, and 138 and 160. The four helices are situated in the N-terminal half of the molecule, consistent with the four-helix bundle observed in the crystal structure of the apoE fragment 1–191 (17).

The HX kinetics of apoE4MM are the same as those for apoE3MM (*SI Appendix, Fig. S3*), despite some self-association of the latter variant in our hands, indicating that the secondary structures are very similar. Helix locations in apoE4MM (by HX) and apoE3MM (by NMR) are compared in Fig. 3 *A* and *B*. The four ~20-residue-long N-terminal helices that form a bundle are similar in both isoforms. The short helices spanning residues 6 to 9 and 12 to 22 in the NMR structure of apoE3MM are not observed by HX, presumably because they are relatively unstable ($P_f < 20$) and exchange before the first experimental time point (0.5 min). CD measurements are also consistent with the existence of some unstable helix structure that is not detected by HX insofar as the total helix content of apoE4MM measured by CD and HX are 58% and 29%, respectively. Much of the shortfall in HX-derived α -helix content arises because the C-terminal helices are also unstable (see *Helix Stability and Dynamics*), although they can be detected by NMR.

Influence of Tetramer Formation on ApoE Secondary Structure. The C-terminal helices in tetrameric WT apoE4 are more stable and can be detected by HX. Helix locations, shown in Fig. 3C, were derived by analysis of the HX kinetics for all peptide fragments spanning the entire length of the protein (*SI Appendix, Fig. S4 and Table S2*). Comparison of Fig. 3 *A* and *C* indicates that the locations of the four bundled N-terminal helices are the same in apoE4 MM and WT. However, in contrast to the case of apoE4MM, the C-terminal domain in WT apoE4 contains a long helical segment that

spans residues 228 to 285 (Fig. 3C). The HX data add up to a total helix content of 56%, which compares well with the CD-derived value of 63%. The finding that self-association of apoE is mediated by the C-terminal domain and involves structural reorganization is consistent with prior studies. Thus, elimination of the C-terminal domain prevents apoE self-association (36), and HX and MS analyses have identified residues in the region 230–270 as playing a critical role in oligomer formation (37, 38). The reorganization of the C-terminal domain upon self-association to form tetramers is likely to involve pairwise interaction of apoE molecules (39) with coiled-coil helix formation (40).

Comparison of Helix Locations in Tetrameric WT ApoE3 and ApoE4.

Measurements at 5 °C where HX is slowed provide more complete kinetic data for comparison of the helix locations in tetrameric WT apoE3 and apoE4, summarized in Fig. 4 (see also *SI Appendix, Figs. S5 and S6 and Tables S3 and S4*). In the case of WT apoE4, the locations of the bundled N-terminal helices are unaltered by cooling from 25 °C to 5 °C (Figs. 3C and 4A). Peptide fragments spanning residue 130 were not obtained in the 5 °C experiments, so the start of helix spanning residues 135 to 165 in this case is inferred from the 25 °C results. There is evidence of fraying of the N-terminal ends of

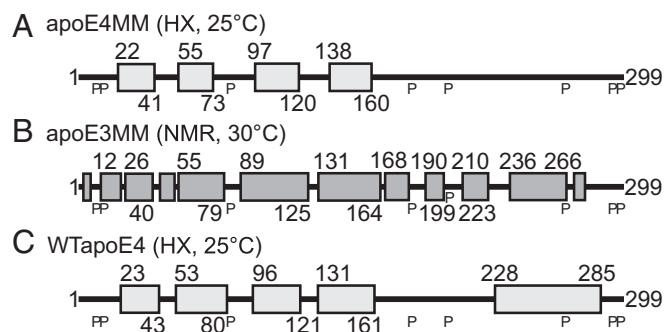


Fig. 3. Comparison of the HX-derived helix locations in lipid-free apoE4 MM and WT apoE4 (*A* and *C*; pD 7.3, 25 °C) and a published NMR structure for apoE3MM (*B*; pH 6.8, 30 °C). The lines represent disordered structure. The positions of proline residues (P), which may perturb α -helix, are marked. The relatively unstable C-terminal helices can be seen by NMR, but they exchange too fast to be seen by HX under the present conditions.

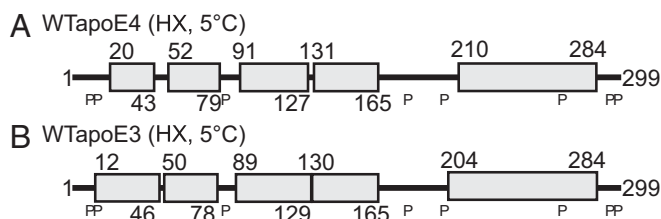


Fig. 4. Comparison of the HX-derived helix locations for lipid-free, tetrameric, (A) WT apoE4 and (B) WT apoE3 at 5 °C (pD 7.3). The lower temperature stabilizes frayed helix ends. The free energy of stabilization of the helices is in the range 4 kcal/mol to 5 kcal/mol for both apoE isoforms (see text for additional details).

certain helices at 25 °C. In particular, the long C-terminal helix starts at residues 210 and 228 at 5 °C and 25 °C, respectively, elongating the unstructured hinge region by 18 amino acids. The total helix content of WT apoE4 at 5 °C and 25 °C is 62% and 56%, respectively; CD indicates ~63% in both cases.

The bundled N-terminal helices are similar but not identical in WT apoE3 and WT apoE4 (Fig. 4). A notable difference is that the first helix spans residues 20 to 43 in apoE4, but it appears to be longer, spanning residues 12 to 46, in apoE3. A helix that spans residues 12 to 20 is apparent in the NMR structure of apoE3MM (Fig. 3B). Evidently, the decreased length of this helix in WT apoE4 is a reflection of the decreased stability of the N-terminal helix bundle domain in this isoform, which contains arginine rather than cysteine at position 112 (41, 42). Similarly, the C-terminal helix appears to be shorter in WT apoE4, spanning residues 210 to 284, compared with 204 to 284 in WT apoE3. It follows that the hinge region separating the N- and C-terminal domains is six residues longer in WT apoE4, which may modify interactions between the two domains.

The differences in HX kinetics for peptide 199–214 in the two isoforms (Fig. 5) provide a direct demonstration of helix destabilization and the altered helix boundary between residues 204 and 210. The unimodal mass spectra and time course of H-to-D exchange show that there is essentially complete lack of protection (Pf < 20) for the apoE4 199 to 214 peptide. Analysis of data in *SI Appendix, Table S3* for overlapping peptides 206–214, 206–216 and 206–218 indicates that protection starts at residue 214 ± 2 in apoE4 (helix starts at residue 210). In contrast, the bimodal mass spectra at early times and time course of H-to-D exchange show that, in the apoE3 199–214 peptide, eight amide hydrogens are unprotected and five are protected (Pf 1,900), consistent with the presence of some stable helical structure. Because peptide 199–205 lack protection (*SI Appendix, Table S4*), it follows that the protected residues are in the span 206 to 214. Analysis of HX data in *SI Appendix, Table S4* for overlapping peptides 199–214, 199–218, 202–218, 206–214, 206–216, and 206–218 indicates that protection starts at residue 208 ± 3 in apoE3 (helix starts at residue 204).

Helix Stability and Dynamics. The Pf values (*SI Appendix, Tables S1–S4*) for the apoE helical segments depicted in Figs. 3 and 4 are consistent with ΔG of helix stabilization in the range 4 kcal/mol to 5 kcal/mol. This same range holds for the N-domain helix bundle in the monomeric and tetrameric states of apoE3 and apoE4 at 5 °C and 25 °C, and is similar to values obtained by urea denaturation measurements with both isoforms (4 kcal/mol to 7 kcal/mol) (15, 43). This stabilization ΔG is consistent with the existence of mutually stabilizing helix–helix interactions in the helix bundle, (31) because individual unsupported α -helices are not stable. The C-terminal helix stabilization ΔG is also 4 kcal/mol to 5 kcal/mol for the tetrameric state; apoE is known to self-associate via the C domain, and intermolecular helix–helix interactions contribute to the stabilization in this case. There are minor fluctuations in stability along the length of the C-terminal helix that extends from about residue 210 to residue 284, but even the presence of proline 267 does not significantly decrease the local stability. However, as is apparent from Fig. 3A and C and reported before, the stability of

the long C-terminal helix is markedly reduced by dissociation of apoE tetramers to monomers (37, 38). In monomeric apoE, the C-terminal helix is not seen by HX, indicating a Pf < 20, which corresponds to a stabilization ΔG < 1.8 kcal/mol and helical structure that is unfolded ~5% of the time (31). This finding agrees with a ΔG of 1.4 kcal/mol to 1.7 kcal/mol measured by urea denaturation for the C domain of monomeric WT apoE3 and E4 (43).

The apoE helix stabilization ΔG of 4 kcal/mol to 5 kcal/mol is similar to that of the related apoA-I molecule (3 kcal/mol to 5 kcal/mol) but significantly lower than values in the range 5 kcal/mol to 10 kcal/mol typically observed for globular proteins (30, 31). The low global stability of the apoE molecule is consistent with high conformational flexibility. The stabilization ΔG corresponds to an unfolding equilibrium constant of $\sim 10^{-3}$, indicating that the apoE helices spend about 0.1% of the time unfolded. Because α -helices are able to fold on a submillisecond time scale, it appears that the apoE helices may well be able to unfold and refold in a timeframe of seconds or less (31). Such dynamic behavior and structural flexibility allows apoE molecules to adapt and bind readily to surfaces of different sizes and shapes.

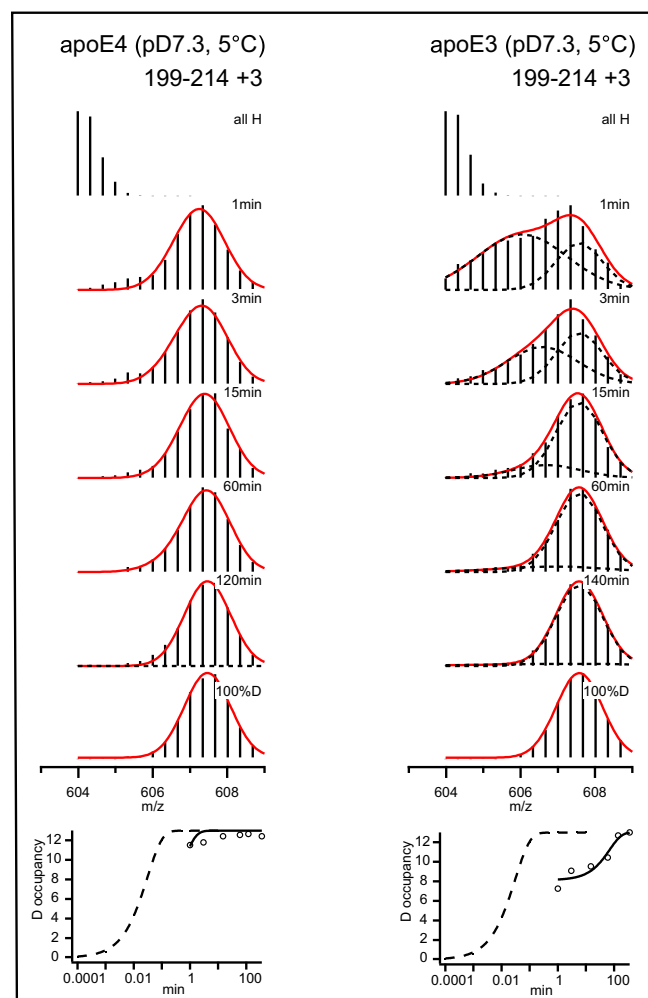


Fig. 5. Comparison of HX kinetics (pD 7.3, 5 °C) of segment spanning residues 199 to 214 in apoE3 and apoE4. This peptide spans Pro202 and therefore contains 13 exchangeable amide hydrogens that can be detected by HX. (Left) Unimodal mass spectra and time course of H-to-D exchange showing lack of protection for the apoE4 199–214 peptide (charge state +3). (Right) Bimodal mass spectra at early times and time course of H-to-D exchange showing protection for five amides in the equivalent apoE3 peptide. Six other peptides agree with this estimate (see *Comparison of Helix Locations in Tetrameric WT ApoE3 and ApoE4*).

Molecular Basis for the Differences in C-Terminal Domain Structure of ApoE3 and ApoE4. The self-association of apoE is mediated by the C-terminal domain (36), and our HX results show that this helical domain is stabilized upon tetramer formation (ΔG stabilization increases from <1.8 kcal/mol to between 4 kcal/mol and 5 kcal/mol). Helix stabilization in the region of residues 204 to 210 is lower in apoE4 tetramer compared with the apoE3 counterpart (Figs. 4 and 5). Prior studies have also established that the C-terminal domain organization is different in apoE3 and apoE4; there is greater solvent exposure of W264 in apoE4 (28) and enhanced hydrophobic surface exposure (reflected by more binding of 8-anilino sulfonic acid) in the C terminal of this isoform (7, 44, 45).

What is the mechanism by which the presence of N-terminal helix bundle-located R112 induces the changes in secondary structure of the separately folded C-terminal domain? Replacement of the neutral and small cysteine side-chain by the charged and bulky arginine side-chain destabilizes the helix bundle in apoE4, as observed in chemical (41) and thermal (42) denaturation studies. Comparison of the crystal structures of the isolated N-terminal domains of the two isoforms indicates that the presence of R112 in apoE4 leads to reorientation of the R61 side-chain in the helix bundle (46). The structure of the apoE tetramer is unknown, but, presumably, accommodation of this reorganized apoE4 helix bundle in the tetramer is different from that of the apoE3 helix bundle containing C112. We propose that, as a consequence, intermolecular C-terminal helix–helix interactions are perturbed, resulting in destabilization of the helical segment spanning residues 204 to 210. There also may be an intramolecular contribution to be considered. Thus, in the monomeric state, the N- and C-terminal domains interact (14), and it is possible that modified intramolecular domain–domain interaction (and length of hinge region) in apoE4 compared with apoE3 (Fig. 6) also contributes to the alteration in structure of the tetramer. The modified domain–domain interaction in apoE4 may be a consequence of the reoriented R61 side-chain modifying the charge distribution in the helix spanning residues 131 to 164, thereby perturbing the structure of the adjacent C-terminal helical residues 271–279 (22, 23). Another contribution to the altered C-terminal domain organization in apoE4 may arise from perturbation of the hinge region by alteration of the hinge–helix bundle interaction through elimination of the R61–T194 hydrogen bond that exists in apoE3 (16) because of the R61 side-chain reorientation in apoE4. In sum, the presence of R112 in apoE4 probably modifies both intermolecular and intramolecular interactions in the tetramer, thereby altering the structure of the tetramer.

Influence of Differences in Secondary Structure on ApoE3 and ApoE4 Functionality. As summarized in the introductory paragraphs, the physiological functions of the apoE molecule involve various binding events that are mediated by amphipathic α -helices located in the N- and C-terminal domains. After dissociation of apoE tetramers [such as occur in plasma HDL-LpE (35)] to the monomeric state (15, 47), the C-terminal helical domain initiates hydrophobic interactions such as binding to lipid and lipoprotein surfaces (7, 44), and to amyloid- β (13, 48). The present HX results prove that the amphipathic α -helix organization in the C-terminal domains of tetrameric WT apoE3 and apoE4 is different and suggest the following explanation for the molecular basis of the enhanced binding of apoE4 in such situations.

The above alterations in conformation must underlie the reduced ability of apoE4 to form tetramers relative to apoE3 (15, 28). Although the structure of dimeric and tetrameric apoE is unknown, the concept that the reduced C-domain helix length in apoE4 (Fig. 6) decreases tetramer stability seems reasonable given that it is well established that truncations of the C-terminal helical region lower the ability of apoE to self-associate (28, 36, 44). The resultant increase of apoE4 monomer/tetramer ratio compared with apoE3 provides more monomer molecules, which, unlike the tetramers, are functional in lipid binding (15, 47). That is, the competition between apo E4 tetramerization and binding to other surfaces is shifted toward the latter. This effect explains the higher measured binding affinity of apoE4 relative to apoE3 for lipid emulsion and VLDL particles (7, 44). The structurally induced differences in the ratio of monomer/tetramer in apoE4 compared with apoE3 lead to subtle alterations in binding ability and varying effects on the kinetics of important catabolic processes that apoE mediates in vivo. First, in the peripheral circulation, the enhanced binding of apoE4 to VLDL particles relative to apoE3 inhibits VLDL lipolysis by lipoprotein lipase. Therefore, at the same apoE expression level, progression down the lipolysis cascade will be relatively limited (8), leading to higher plasma cholesterol levels and, potentially, the increased incidence of cardiovascular disease associated with apoE4 (6). Second, in the brain, the enhanced binding of apoE4 to amyloid- β oligomers can alter the kinetics of aggregation by inhibiting growth and nucleation on the pathway to forming fibrils (13). This effect may promote pathogenesis by, for example, leading to greater accumulation of the cytotoxic oligomeric forms of amyloid- β . Overall, the current findings suggest that the pathological effects associated with apoE4 may be offset by treatments that enhance its tetramer-forming ability to that of apoE3. It is possible that small-molecule “structure correctors” that bind to apoE4 and make it behave more like apoE3 (49, 50) work in this fashion.

Materials and Methods

Human apoE3 and apoE4 were expressed in *Escherichia coli* as thioredoxin fusion proteins and isolated and purified as described previously (19, 20). Cleavage with thrombin leaves the target apoE with two extra amino acids, glycine and serine (designated residues -2, -1), at the N terminus that do not significantly alter the properties of the protein. The QuikChange site-directed mutagenesis kit (Stratagene) was used to introduce the mutations F257AWW264RV269AL279QV287E into the C-terminal domain and generate monomeric variants of apoE3 and apoE4 (14). The apoE preparations were at least 95% pure as assessed by SDS/PAGE. ApoE samples used for the HX experiments were freshly dialyzed at 4 °C from a 6 M GdmCl and 10 mM DTT solution into a buffer solution. Protein concentrations were determined by absorbance at 280 nm. The average α -helix contents of the apoE variants were determined by CD spectra at room temperature using a Jasco J-810 spectropolarimeter (24) and analyzed as described previously (28, 30).

HX MS methods (51–54) were applied to determine the locations, stabilities, and dynamics of α -helical segments within the apoE variants. In brief, HX was initiated by diluting apoE samples into D₂O buffer, and the kinetics of H-to-D exchange throughout the protein was determined by a fragment separation method (55) and MS analysis (30, 31). Time-dependent H-to-D exchange was measured at the segment level for ~115 peptide fragments (Fig. 1A). Formation of hydrogen bonds by the amide groups of amino acids located in α -helix protects them from exchange with water hydrogens, and exchange only occurs when the protecting H bond is transiently severed in some dynamic structural “opening” reaction (30). Because secondary structure in apoE molecules is limited to α -helix or helical bundles, the determination of protected amides in an apoE molecule indicates helix location. Comparison of results for overlapping

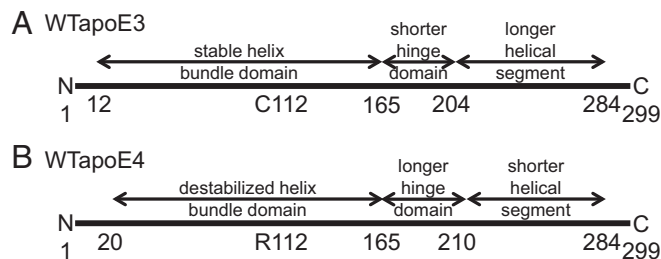


Fig. 6. Diagram summarizing the structural differences between lipid-free apoE3 and apoE4 and the functional consequences of these variations. The point substitution C112R that distinguishes apoE4 from apoE3 destabilizes the N-terminal helix bundle domain, inducing helix shortening between amino acids 12 and 20 in this domain and residues 204 and 210 in the C-terminal domain of apoE4. In the monomeric state, the latter change in conformation is presumably mediated by interaction between the N- and C-terminal domains, which are linked by a hinge region. In the tetrameric state, intermolecular interactions can contribute to the helix destabilization between residues 12 and 20 and 204 and 210 in apoE4. These conformational changes reduce the ability of apoE4 to form tetramers, thereby raising the concentration of monomer available for binding, leading to the higher-affinity binding of apoE4 compared with apoE3 (see text for further details).

peptides often produces resolution better than the single-fragment level. When exchange depends on cooperative helix unfolding, the degree of HX protection measures helix stability. The observed HX rate curve was compared with a reference rate curve calculated assuming the fragment to be in a dynamically disordered random coil state where amide hydrogens are not protected against exchange with water (56). The Pf, which is the ratio (reference rate/observed rate), was used to

calculate the free energy of HX ($\Delta G_{\text{HX}} = RT \ln Pf$) helix unfolding (30, 31). Further details are in *SI Appendix*.

ACKNOWLEDGMENTS. This work was supported by research grants from National Institutes of Health (Grant GM031847), National Science Foundation (Grant MCB1020649), and The Mathers Charitable Foundation.

- Weisgraber KH (1994) Apolipoprotein E: Structure-function relationships. *Adv Protein Chem* 45:249–302.
- Segrest JP, et al. (1992) The amphipathic helix in the exchangeable apolipoproteins: A review of secondary structure and function. *J Lipid Res* 33(2):141–166.
- Davignon J, Gregg RE, Sing CF (1988) Apolipoprotein E polymorphism and atherosclerosis. *Arteriosclerosis* 8(1):1–21.
- Mahley RW, Ji ZS (1999) Remnant lipoprotein metabolism: Key pathways involving cell-surface heparan sulfate proteoglycans and apolipoprotein E. *J Lipid Res* 40(1):1–16.
- Mahley RW, Huang Y, Rall SC, Jr (1999) Pathogenesis of type III hyperlipoproteinemia (dysbetalipoproteinemia). Questions, quandaries, and paradoxes. *J Lipid Res* 40(11):1933–1949.
- Phillips MC (2014) Apolipoprotein E isoforms and lipoprotein metabolism. *IUBMB Life* 66(9):616–623.
- Nguyen D, et al. (2010) Molecular basis for the differences in lipid and lipoprotein binding properties of human apolipoproteins E3 and E4. *Biochemistry* 49(51):10881–10889.
- Li H, et al. (2013) Molecular mechanisms responsible for the differential effects of apoE3 and apoE4 on plasma lipoprotein-cholesterol levels. *Arterioscler Thromb Vasc Biol* 33(4):687–693.
- Hauser PS, Narayanaswami V, Ryan RO (2011) Apolipoprotein E: From lipid transport to neurobiology. *Prog Lipid Res* 50(1):62–74.
- Hauser PS, Ryan RO (2013) Impact of apolipoprotein E on Alzheimer's disease. *Curr Alzheimer Res* 10(8):809–817.
- Huang Y, Mahley RW (2014) Apolipoprotein E: Structure and function in lipid metabolism, neurobiology, and Alzheimer's diseases. *Neurobiol Dis* 72(Pt A):3–12.
- Joshi PK, et al. (2016) Variants near CHRNA3/5 and APOE have age- and sex-related effects on human lifespan. *Nat Commun* 7:11174.
- Garai K, Vergheze PB, Baban B, Holtzman DM, Frieden C (2014) The binding of apolipoprotein E to oligomers and fibrils of amyloid- β alters the kinetics of amyloid aggregation. *Biochemistry* 53(40):6323–6331.
- Zhang Y, et al. (2007) A monomeric, biologically active, full-length human apolipoprotein E. *Biochemistry* 46(37):10722–10732.
- Mizuguchi C, et al. (2014) Fluorescence study of domain structure and lipid interaction of human apolipoproteins E3 and E4. *Biochim Biophys Acta* 1841(12):1716–1724.
- Chen J, Li Q, Wang J (2011) Topology of human apolipoprotein E3 uniquely regulates its diverse biological functions. *Proc Natl Acad Sci USA* 108(36):14813–14818.
- Wilson C, Wardell MR, Weisgraber KH, Mahley RW, Agard DA (1991) Three-dimensional structure of the LDL receptor-binding domain of human apolipoprotein E. *Science* 252(5014):1817–1822.
- Garai K, Frieden C (2010) The association–dissociation behavior of the ApoE proteins: Kinetic and equilibrium studies. *Biochemistry* 49(44):9533–9541.
- Mizoguchi C, et al. (2001) Lipid binding-induced conformational change in human apolipoprotein E. Evidence for two lipid-bound states on spherical particles. *J Biol Chem* 276(44):40949–40954.
- Nguyen D, Dhanasekaran P, Phillips MC, Lund-Katz S (2009) Molecular mechanism of apolipoprotein E binding to lipoprotein particles. *Biochemistry* 48(13):3025–3032.
- Saito H, Lund-Katz S, Phillips MC (2004) Contributions of domain structure and lipid interaction to the functionality of exchangeable human apolipoproteins. *Prog Lipid Res* 43(4):350–380.
- Frieden C, Garai K (2012) Structural differences between apoE3 and apoE4 may be useful in developing therapeutic agents for Alzheimer's disease. *Proc Natl Acad Sci USA* 109(23):8913–8918.
- Frieden C, Garai K (2013) Concerning the structure of apoE. *Protein Sci* 22(12):1820–1825.
- Saito H, et al. (2003) Domain structure and lipid interaction in human apolipoproteins A-I and E, a general model. *J Biol Chem* 278(26):23227–23232.
- Dong LM, Weisgraber KH (1996) Human apolipoprotein E4 domain interaction. Arginine 61 and glutamic acid 255 interact to direct the preference for very low density lipoproteins. *J Biol Chem* 271(32):19053–19057.
- Frieden C (2015) ApoE: The role of conserved residues in defining function. *Protein Sci* 24(1):138–144.
- Nguyen D, et al. (2014) Influence of domain stability on the properties of human apolipoprotein E3 and E4 and mouse apolipoprotein E. *Biochemistry* 53(24):4025–4033.
- Sakamoto T, et al. (2008) Contributions of the carboxyl-terminal helical segment to the self-association and lipoprotein preferences of human apolipoprotein E3 and E4 isoforms. *Biochemistry* 47(9):2968–2977.
- Drury J, Narayanaswami V (2005) Examination of lipid-bound conformation of apolipoprotein E4 by pyrene excimer fluorescence. *J Biol Chem* 280(15):14605–14610.
- Sevugan Chetty P, et al. (2012) Apolipoprotein A-I helical structure and stability in discoidal high-density lipoprotein (HDL) particles by hydrogen exchange and mass spectrometry. *Proc Natl Acad Sci USA* 109(29):11687–11692.
- Chetty PS, et al. (2009) Helical structure and stability in human apolipoprotein A-I by hydrogen exchange and mass spectrometry. *Proc Natl Acad Sci USA* 106(45):19005–19010.
- Chetty PS, et al. (2013) Comparison of apoA-I helical structure and stability in discoidal and spherical HDL particles by HX and mass spectrometry. *J Lipid Res* 54(6):1589–1597.
- Chetty PS, et al. (2012) Effects of the Iowa and Milano mutations on apolipoprotein A-I structure and dynamics determined by hydrogen exchange and mass spectrometry. *Biochemistry* 51(44):8993–9001.
- Yokoyama S, Kawai Y, Tajima S, Yamamoto A (1985) Behavior of human apolipoprotein E in aqueous solutions and at interfaces. *J Biol Chem* 260(30):16375–16382.
- Krimbou L, Marcil M, Chiba H, Genest J, Jr (2003) Structural and functional properties of human plasma high density-sized lipoprotein containing only apoE particles. *J Lipid Res* 44(5):884–892.
- Westerlund JA, Weisgraber KH (1993) Discrete carboxyl-terminal segments of apolipoprotein E mediate lipoprotein association and protein oligomerization. *J Biol Chem* 268(21):15745–15750.
- Gau B, Garai K, Frieden C, Gross ML (2011) Mass spectrometry-based protein footprinting characterizes the structures of oligomeric apolipoprotein E2, E3, and E4. *Biochemistry* 50(38):8117–8126.
- Huang RY, Garai K, Frieden C, Gross ML (2011) Hydrogen/deuterium exchange and electron-transfer dissociation mass spectrometry determine the interface and dynamics of apolipoprotein E oligomerization. *Biochemistry* 50(43):9273–9282.
- Fabilane CS, et al. (2016) Mechanism of lipid binding of human apolipoprotein E3 by hydrogen/deuterium exchange/mass spectrometry and fluorescence polarization. *Protein Pept Lett* 23(4):404–413.
- Choy N, Raussens V, Narayanaswami V (2003) Inter-molecular coiled-coil formation in human apolipoprotein E C-terminal domain. *J Mol Biol* 334(3):527–539.
- Morrow JA, et al. (2000) Differences in stability among the human apolipoprotein E isoforms determined by the amino-terminal domain. *Biochemistry* 39(38):11657–11666.
- Acharya P, et al. (2002) Comparison of the stabilities and unfolding pathways of human apolipoprotein E isoforms by differential scanning calorimetry and circular dichroism. *Biochim Biophys Acta* 1584(1):9–19.
- Garai K, Baban B, Frieden C (2011) Self-association and stability of the ApoE isoforms at low pH: Implications for ApoE-lipid interactions. *Biochemistry* 50(29):6356–6364.
- Saito H, et al. (2003) Effects of polymorphism on the lipid interaction of human apolipoprotein E. *J Biol Chem* 278(42):40723–40729.
- Tanaka M, et al. (2006) Effect of carboxyl-terminal truncation on structure and lipid interaction of human apolipoprotein E4. *Biochemistry* 45(13):4240–4247.
- Dong LM, et al. (1994) Human apolipoprotein E. Role of arginine 61 in mediating the lipoprotein preferences of the E3 and E4 isoforms. *J Biol Chem* 269(35):22358–22365.
- Garai K, Baban B, Frieden C (2011) Dissociation of apolipoprotein E oligomers to monomer is required for high-affinity binding to phospholipid vesicles. *Biochemistry* 50(13):2550–2558.
- Strittmatter WJ, et al. (1993) Binding of human apolipoprotein E to synthetic amyloid beta peptide: Isoform-specific effects and implications for late-onset Alzheimer disease. *Proc Natl Acad Sci USA* 90(17):8098–8102.
- Chen HK, et al. (2012) Small molecule structure correctors abolish detrimental effects of apolipoprotein E4 in cultured neurons. *J Biol Chem* 287(8):5253–5266.
- Mondal T, et al. (2016) ApoE: In vitro studies of a small molecule effector. *Biochemistry* 55(18):2613–2621.
- Kan ZY, Mayne L, Chetty PS, Englander SW (2011) ExMS: Data analysis for HX-MS experiments. *J Am Soc Mass Spectrom* 22(11):1906–1915.
- Kan ZY, Walters BT, Mayne L, Englander SW (2013) Protein hydrogen exchange at residue resolution by proteolytic fragmentation mass spectrometry analysis. *Proc Natl Acad Sci USA* 110(41):16438–16443.
- Mayne L, et al. (2011) Many overlapping peptides for protein hydrogen exchange experiments by the fragment separation-mass spectrometry method. *J Am Soc Mass Spectrom* 22(11):1898–1905.
- Walters BT, Ricciuti A, Mayne L, Englander SW (2012) Minimizing back exchange in the hydrogen exchange-mass spectrometry experiment. *J Am Soc Mass Spectrom* 23(12):2132–2139.
- Englander JJ, Rogero JR, Englander SW (1985) Protein hydrogen exchange studied by the fragment separation method. *Anal Biochem* 147(1):234–244.
- Bai Y, Milne JS, Mayne L, Englander SW (1993) Primary structure effects on peptide group hydrogen exchange. *Proteins* 17(1):75–86.